Experimental Demonstration of the Vibrational Stabilization Phenomenon in Bio-inspired Flying Robots

Haithem Taha[1], Mohammadali Kiani[1] and Joel Navarro[2]

***Abstract*—Bio-inspired flying robots (BIFRs) are micro-air-vehicles that use biomimetic actuation (oscillatory flapping wing) for lift, propulsion, and control. The dynamic behavior of these bio-inspired systems is quite intricate to study as it is typically described by a multi-body, multi-time-scale, nonlinear, time-varying dynamical system. However, this rich dynamics lead to unconventional stabilization mechanisms whose study essentially necessitates a mathematically rigorous analysis. Our recent efforts using differential geometric control theory revealed a *vibrational stabilization* mechanism induced on the body pitching due to the interaction between the fast wing flapping dynamics and the slow body dynamics. In this effort, we construct an experimental setup allowing for two degrees of freedom for the body; vertical motion and pitching motion. The objective is to experimentally verify and demonstrate the vibrational stabilization phenomenon in insect flight and its mimicking BIFRs.**

***Index Terms*—Aerial Systems: Mechanics and Control, Biomimetics, Dynamics**

I. Introduction

BIO-INSPIRED flying robots (BIFRs) or flapping-wing micro-air-vehicles represent a rich dynamical system with unconventional dynamical behavior that caught the attention of biologists and engineers over the last two decades. The multi-body dynamics of BIFRs is typically described by nonlinear, time-periodic (NLTP) models. Moreover, the fast oscillatory wing motion and its associated inertial and aerodynamic loads interact with the relatively slower body motion resulting in a multi-time-scale dynamical system. These features lead to interesting unconventional balance and stability characteristics, which necessitate a mathematically rigorous analysis to study.

In order to analyze the complex dynamics of BIFRs, most of the research efforts adopted the averaging assumption [1–6]; that is, they assumed that the body's response is mainly due to the cycle-averaged aerodynamic loads. However, this assumption obscures the beautiful unconventional dynamical behavior of these bio-inspired systems, as shown by the recent efforts of Taha et al. [7, 8] by rigorously combining averaging and differential geometric control tools. It has been shown that, for hovering insects and BIFRs with a relatively small flapping frequency (e.g., hawkmoth and cranefly), in spite of the large separation between the system's two time scales (30 for the hawkmoth and 50 for the cranefly), there is a strong interaction between the high-frequency flapping dynamics and the low-frequency body dynamics that results in an unconventional stabilization mechanism; vibrational stabilization. This interaction is essentially neglected when direct averaging is used [7–9].

Vibrational stabilization is an open loop stabilization technique of an unstable equilibrium via the application of a sufficiently high-amplitude, high-frequency periodic forcing. For example, the unstable equilibrium of the inverted pendulum gains asymptotic stability when the pivot is oscillating vertically at a sufficiently high frequency. Direct averaging of the simple equations governing the dynamics of the Kapitza pendulum (inverted pendulum whose pivot is subject to a vertical oscillation [10, 11]) showed no stabilization due to the pivot vibration. However, appropriate averaging techniques clearly show a vibrationally-induced stabilizing stiffness [12].

While many research reports (e.g., [2–4, 13–20]) concluded an unstable flight dynamics for hovering insects and BIFRs; mainly due to lack of pitch stiffness, the recent efforts by Taha et al. [7, 8, 21, 22] showed an induced vibrational stabilization mechanism in the form of pitch stiffness on the flight dynamics of these bio-inspired robots. In this paper, we focus mainly on the experimental demonstration of such a phenomenon in insect flight and BIFRs.

II. Experimental Setup

A. Performance Characterization

In order to avoid the many problems associated with free flight and to have a better focus on verifying the vibrational stabilization phenomenon, we construct an experimental setup that allows for only two degrees of freedom (DOFs) for the body of the BIFR; vertical motion and pitching motion. Imagine a simple pendulum with its mass replaced by a BIFR, as shown in the schematic in Fig. 1(a). The hovering equilibrium is then achieved when the pendulum's rod becomes horizontal, as shown in the real picture of our realization presented in Fig. 1(b). This system represents the simplest configuration with a single DOF (the pendulum angle γ) that mimics the vertical motion of the body.

Manuscript received: September, 6, 2017; Accepted November, 4, 2017.

This paper was recommended for publication by Editor J. Roberts upon evaluation of the Associate Editor and Reviewers' comments. The first author is thankful to the support of the National Science Foundation grant CMMI-1709746.

[1]H. Taha and M. Kiani are with School of Engineering, Mechanical and Aerospace Engineering Department, University of California, Irvine, CA hetaha@uci.edu, mkiani@uci.edu

[2]J. Navarro is with School of Engineering, Aerodynamic and Energy Department , Ecole Nationale Superieure de Mcanique et d'Aerotechnique, Chasseneuil du Poitou, France joel.navarro@sfr.fr This work is performed at UCI.

Digital Object Identifier (DOI): see top of this page.

This article has been accepted for publication in a future issue of this journal, but has not been fully edited. Content may change prior to final publication. Citation information: DOI 10.1109/LRA.2017.2778759, IEEE Robotics and Automation Letters

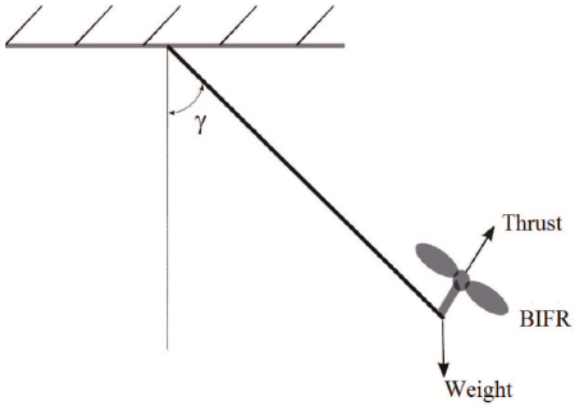

(a) A Pendulum-BIFR Schematic.

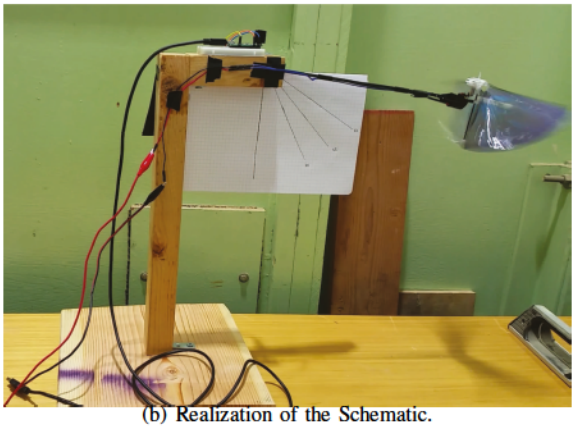

(b) Realization of the Schematic.

Fig. 1: The experimental setup of a pendulum-like BIFR.

This pendulum-like setup is preferred in comparison to the Wood's Harvard Robofly [23] (moving along vertical rails), which was used to prove the concept of BIFRs. Note that for the latter configuration, if the flapping amplitude/frequency is slightly deviated from the hovering balance requirement, the BIFR will experience a vertical climb/descent with some mean velocity. In contrast, because of the gravitational spring action provided by the pendulum configuration, any deviation from the hovering balance requirement results in a slightly different equilibrium *position* γ_e. In addition, measurement of this equilibrium pendulum angle γ_e is easily achieved using a Gravity 360 Degree Hall Angle Sensor [24] and provides a measure for the generated thrust from the BIFR as the flapping frequency changes, according to the balance equation

$$F_T = \left(m_{\text{BIFR}} + \frac{1}{2} m_{\text{rod}} \right) g \sin \gamma_e,$$

where F_T is the cycle-averaged generated thrust force, m_{BIFR} is the mass of the BIFR (13 gm), m_{rod} is the mass of the pendulum's rod (1.8 gm), and g is the gravitational acceleration. The power supply in the lab already provides information about the cycle-averaged total power consumption P. In addition, as the applied voltage is increased, the flapping frequency increases. At each given voltage, a video is recorded at a rate of 240 frame per second. The time stamp of each video is analyzed to obtain an estimate for the flapping frequency (the average flaps per second). As such, the performance characteristics of the BIFR is determined and presented in Fig. 2.

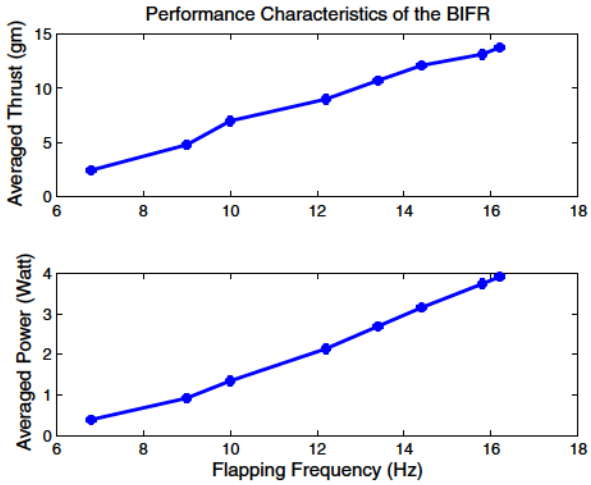

Fig. 2: Performance characteristics of the used BIFR.

The adopted BIFR is an off-the-shelf flapping bird [25] whose wings are highly flexible wings that flap in a vertical stroke plane resulting in a good thrust producing capability at zero forward speed (i.e., at the hovering position). This BIFR (shown in Fig. 3(a)) is adapted for the current experimental setup as shown in Fig. 3(b); only the wings and the flapping mechanism are retained while the body and motor are replaced. Of particular importance is the replacement of the driving motor with a stronger motor [26] that allows operating at higher flapping frequencies, which is necessary for the demonstration of vibrational stabilization.

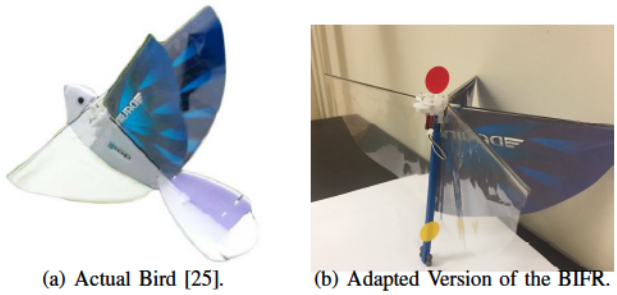

(a) Actual Bird [25]. (b) Adapted Version of the BIFR.

Fig. 3: The actual and adapted BIFRs.

B. Pitching Dynamics

A pin (hinge) connection is introduced between the body of the BIFR and the pendulum's rod to allow for body pitching θ, as shown in Fig. 4. The response of the pitching angle is measured using a digital camera and an image processing algorithm (e.g., [27]). As shown in Figs. 3(b),4, the nose and tail of the BIFR are marked with different colors. Then, a simple algorithm is implemented in Visual Studio C++, exploiting the image processing library OpenCV, to detect these circular stickers from video recordings and determine the angle between the line connecting these two marks and

This article has been accepted for publication in a future issue of this journal, but has not been fully edited. Content may change prior to final publication. Citation information: DOI 10.1109/LRA.2017.2778759, IEEE Robotics and Automation Letters

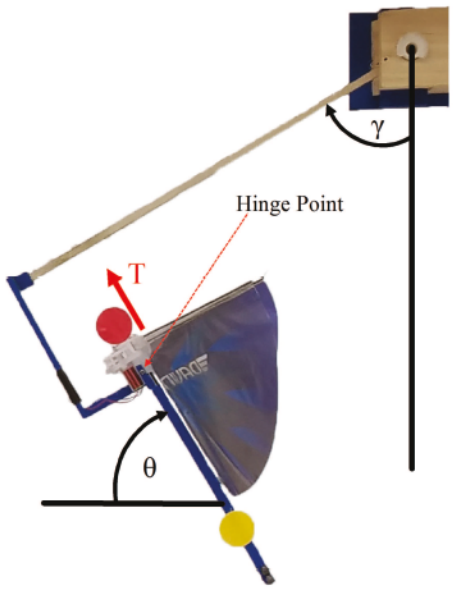

Fig. 4: Two-DOF BIFR Experimental Setup.

the horizontal (i.e. θ) at each time stamp with a sampling frequency of 50 ms.

Because the line of action of the thrust force is above the body longitudinal axis and consequently hinge point, there is an unbalanced pitching moment which will preclude equilibria. Therefore, we added four split shot size lead of 3g total weight near the tail of the BIFR, as shown in Figs. 3(b),4 (the black dots near tail) to shift the center of gravity of the BIFR backward along the longitudinal axis. As such, the pitching moment at the hinge point due to the weight will balance that of the thrust force according to the balance equation

$$F_T e_T = m_{\text{BIFR}} g e_g \cos\theta_e,$$

where e_T and e_g are the offsets of the thrust and gravity forces, respectively, from the hinge point, and θ_e is the equilibrium value of the pitching angle. At zero applied voltage (zero thrust force), the BIFR is standing vertically ($\theta_e = 90°$) at the bottom position ($\gamma_e = 0°$) of the pendulum. As the voltage and consequently the flapping frequency increase, the body moves upward along the circular path of the pendulum (i.e., γ increases) and tilts forward towards the horizontal attitude (i.e., θ decreases), as shown in Fig. 4. It is noteworthy that most insects have their center of gravity behind the hinge location along their longitudinal axis and achieve hovering equilibria at body inclination with respect to the horizontal (i.e., θ_e) around 50° [14, 28]; i.e., similar to the current setup.

III. Demonstration of Vibrational Stabilization

Having established equilibrium, studying stability comes promptly. It is noteworthy that most research reports concluded instability of insects and BIFRs at hover due to lack of pitch stiffness [4, 14, 17–20, 29–31]. Hence, it has been believed that insects and their man-made BIFRs have to employ feedback to stabilize their flight during hover. While this may indeed be true, these studies mostly neglected the potential of the natural high-frequency oscillatory flapping motion to induce vibrational stabilization [7, 8]. To experimentally verify and demonstrate such a phenomenon in the BIFRs, we apply different voltages to the motor driving the flapping mechanism to attain different equilibrium positions (γ_e and θ_e) at different flapping frequencies, thanks to the pendulum configuration and to the stronger motor. We then measure the response of the pendulum angle γ and the body pitching angle θ, as explained above, at each operating frequency.

Figure 5 shows the response of the BIFR system at a flapping frequency of $\sim$ 12Hz (corresponding to 1.94 Volt). At this low flapping frequency, the BIFR barely goes up ($\gamma_e \sim 24°$) and the equilibrium pitching angle is quite large ($\theta_e \sim 76°$). The response is found to be unstable as shown in the figure, even without giving a disturbance; the oscillatory wing motion naturally provides a sufficient disturbance.

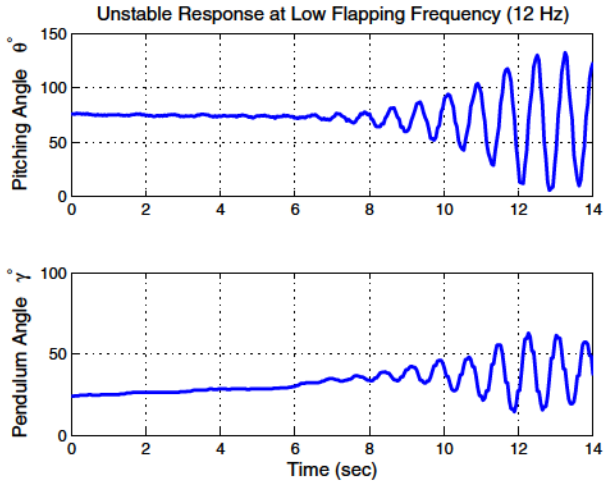

Fig. 5: BIFR unstable response at relatively low flapping frequency ($\sim$ 12Hz).

Figure 6 shows the response of the BIFR system as the applied voltage (flapping frequency) is manually increased from 1V to 3V. The bird rises up towards the hovering position (γ goes from 20° to 60° and θ changes from 77° to 62°). It is clear that the BIFR response experiences instability during the transition period and becomes stable beyond a certain pendulum angle (i.e., flapping frequency). We apply fixed different voltages (corresponding to different flapping frequencies) and observe the system response at each case. The threshold flapping frequency below which the BIFR response is unstable and beyond which it is naturally stabilized is found to be 15Hz. It is envisaged that this threshold should be related to the system's natural frequency (1.4Hz). That is, the stabilization-threshold ratio between the periodic forcing frequency and the system's natural frequency is found to be 10.7 for the current setup. Seeking a universal value for such a ratio is quite important and is suggested for future work.

Figure 7 shows the response of the BIFR system at a relatively high flapping frequency of $\sim$ 18Hz (corresponding to 3 Volt). At this relatively high flapping frequency, the BIFR system is almost at the hovering position ($\gamma_e \sim 85°$) and the equilibrium pitching angle $\theta_e \sim 50°$ is close to the natural

This article has been accepted for publication in a future issue of this journal, but has not been fully edited. Content may change prior to final publication. Citation information: DOI 10.1109/LRA.2017.2778759, IEEE Robotics and Automation Letters

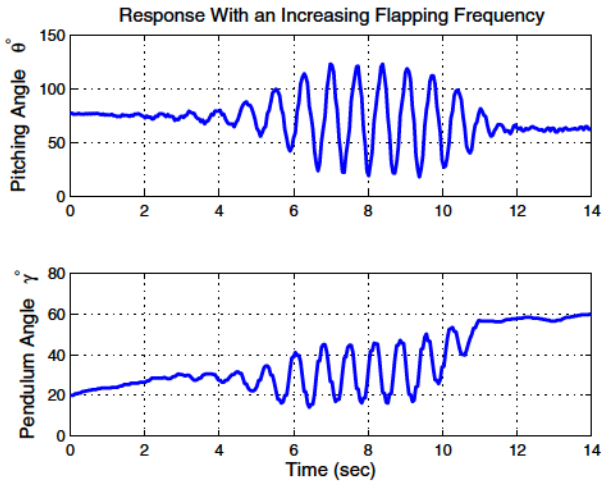

Fig. 6: BIFR response as the flapping frequency is being manually increased.

values observed in nature for hovering insects [14, 28]. Clearly, the response is stable. Even when a relatively large disturbance ($\Delta\theta \sim 50°$) is applied at $t = 8.6$ sec, the system goes back to its equilibrium periodic orbit (i.e., the hovering periodic orbit).

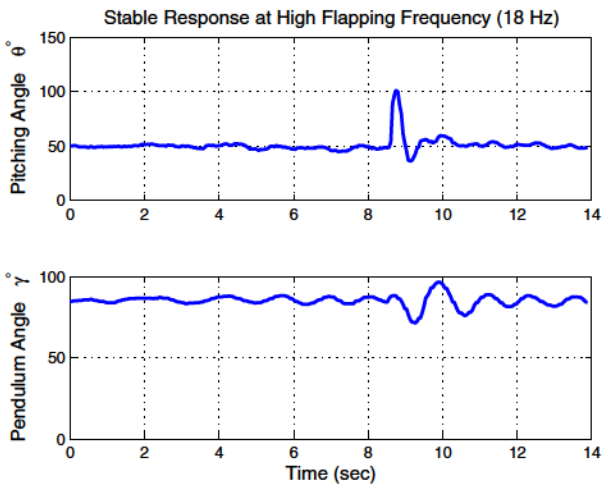

Fig. 7: BIFR stable response at relatively high flapping frequency ($\sim$ 18Hz).

So far, it can be concluded that the response of BIFRs (particularly the body pitch response) is naturally (without feedback) stabilized beyond a certain threshold of flapping frequency. This fact conforms well with the vibrational stabilization phenomenon [10, 11, 32, 33] and suggests that the observed natural stabilization at high frequencies is a vibrational stabilization phenomenon. However, one might argue that because the intricate dynamics of the system, the frequency not only affects stability, but also balance/equilibrium; obviously increasing the frequency leads to a different equilibrium, which may or may not have similar stability characteristics to equilibria corresponding to low frequencies. To show that the induced stabilizing mechanism is indeed a vibrational stabilization one that is mainly due to the time-periodic nature of the driving aerodynamic thrust force and not because of operating at a different equilibrium, we construct a replica of the experimental setup with the BIFR being replaced by a small propeller revolving with a constant speed, as shown in Fig. 8. The main difference is that the BIFR setup produces a periodic thrust force, and consequently a time-periodic dynamics allowing for vibrational stabilization, while the propeller setup produces a constant thrust force, and consequently a time-invariant dynamics leaving no room for vibrational stabilization.

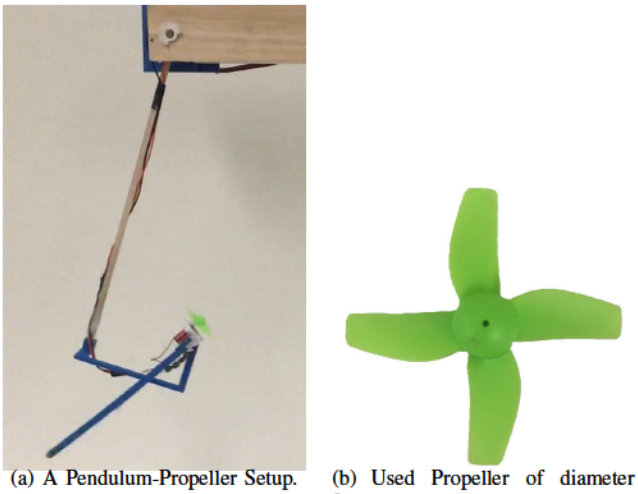

(a) A Pendulum-Propeller Setup. (b) Used Propeller of diameter 3mm.

Fig. 8: A Two-DOF Pendulum-Propeller Setup.

Using split shot size lead, we managed to match the weight and inertia of the propeller system with the BIFR system. Figure 9 shows the response of the two-DOF propeller-pendulum system at a relatively small propeller speed (i.e., at a small pendulum equilibrium angle $\gamma_e \sim 9°$). Clearly, the response is exponentially unstable. Increasing the applied voltage to attain higher pendulum equilibrium angles (closer to the hovering position) worsens the stability characteristics so much that the system structure becomes prone to breaking.

IV. Conclusion

An experimental setup is constructed to study the flight dynamics of a bio-inspired flapping robot that mimics the flight of some insect and birds. The setup allows for two degrees of freedom for the body; vertical motion and pitching motion. The goal was to verify whether such species and their man-mad counterparts exploit the vibrational stabilization phenomenon in their flight, particularly at the hovering position. Recalling that vibrational stabilization is an *open loop* stabilization technique due to the application of a *sufficiently high frequency periodic forcing*, we studied the stability of the system at different flapping frequencies. It was found that the system is naturally (without feedback) stabilized beyond a certain threshold of the flapping frequency (15Hz, equivalently 10.7 times the system's natural frequency, in the current setup), which conforms with the vibrational stabilization phenomenon. Moreover, we constructed a replica of the system

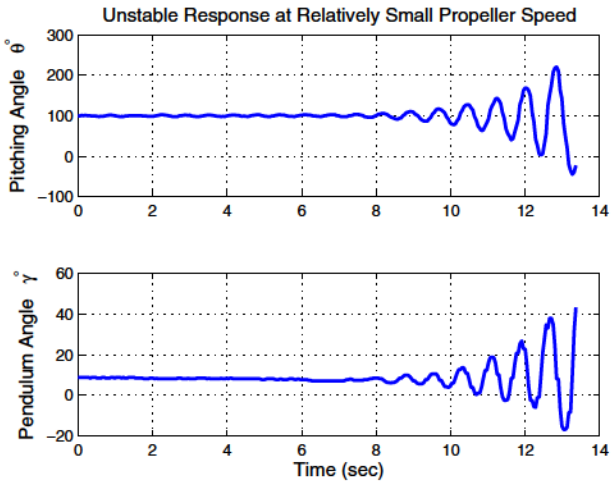

Fig. 9: Unstable Response of the Two-DOF Propeller-Pendulum System.

replacing the flapping bird with a propeller that revolves at a constant speed to check whether the induced stabilization at high frequencies is mainly due to periodicity of the driving force (i.e., a vibrational stabilization) or not. It was found that the propeller system replica is unstable at all applied voltages and becomes even more unstable at larger applied voltages (i.e., when it comes closer to the hovering position). Finally, it is concluded that bio-inspired flapping robots, indeed, enjoy vibrational stabilization.

REFERENCES

[1] A. L. R. Thomas and G. K. Taylor, "Animal flight dynamics i. stability in gliding flight." *Journal of Theoretical Biology*, vol. 212, no. 1, pp. 399–424, 2001.

[2] G. K. Taylor and A. L. R. Thomas, "Animal flight dynamics ii. longitudinal stability in flapping flight," *Journal of Theoretical Biology*, vol. 214, 2002.

[3] ——, "Dynamic flight stability in the desert locust," *Journal of Theoretical Biology*, vol. 206, no. 6, pp. 2803–2829, 2003.

[4] M. Sun and Y. Xiong, "Dynamic flight stability of a hovering bumblebee." *Journal of Experimental Biology*, vol. 208, no. 3, pp. 447–459, 2005.

[5] D. B. Doman, M. W. Oppenheimer, and D. O. Sigthorsson, "Wingbeat shape modulation for flapping-wing micro-air-vehicle control during hover," *Journal of Guidance, Control and Dynamics*, vol. 33, no. 3, pp. 724–739, 2010.

[6] M. W. Oppenheimer, D. B. Doman, and D. O. Sigthorsson, "Dynamics and control of a biomimetic vehicle using biased wingbeat forcing functions," *Journal Guidance, Control and Dynamics*, vol. 34, no. 1, pp. 204–217, 2011.

[7] H. E. Taha, S. Tahmasian, C. A. Woolsey, A. H. Nayfeh, and M. R. Hajj, "The need for higher-order averaging in the stability analysis of hovering mavs/insects," vol. 10, no. 1, p. 016002, selected in the Bioinspiration & Biomimetics Highlights of 2015.

[8] H. E. Taha, A. H. Nayfeh, and M. R. Hajj, "Effect of the aerodynamic-induced parametric excitation on the longitudinal stability of hovering mavs/insects," *Nonlinear Dynamics*, vol. 78, no. 4, pp. 2399–2408, 2014.

[9] A. H. Nayfeh and D. T. Mook, *Nonlinear Oscillations*. John Wiley and Sons, Inc., 1979.

[10] P. L. Kapitza, "Pendulum with a vibrating suspension," *Uspekhi Fiz. Nauk*, vol. 44, no. 1, pp. 7–20, 1951.

[11] ——, "Dynamical stability of a pendulum when its point of suspension vibrates," *Collected Papers by PL Kapitza*, vol. 2, pp. 714–725, 1965.

[12] J. Baillieul and B. Lehman, "Open-loop control using oscillatory inputs," *CRC Control Handbook*, pp. 967–980, 1996.

[13] G. K. Taylor and R. Zbikowski, "Nonlinear time periodic models of the longitudinal flight dynamics of desert locusts," *J. Roy. Soc. Interface*, vol. 1, no. 3, p. 197221, 2005.

[14] M. Sun, J. Wang, and Y. Xiong, "Dynamic flight stability of hovering insects," *Acta Mechanica Sinica*, vol. 23, no. 3, pp. 231–246, 2007.

[15] M. Richter and M. Patil, "Influence of wing flexibility on the stability of flapping flight," in *AIAA Atmospheric Flight Mechanics Conference*, 2010, pp. 2–5.

[16] J. M. Dietl and E. Garcia, "Stability in ornithopter longitudinal flight dynamics," *Journal of Guidance, Control and Dynamics*, vol. 31, no. 4, pp. 1157–1162, 2008.

[17] N. Gao, H. Aono, and H. Liu, "A numerical analysis of dynamic flight stability of hawkmoth hovering," *Journal of Biomechanical Science and Engineering*, vol. 4, no. 1, pp. 105–116, 2009.

[18] W. Su and C. E. S. Cesnik, "Flight dynamic stability of a flapping wing micro air vehicle in hover." AIAA-Paper 2011-2009.

[19] I. Faruque and J. S. Humbert, "Dipteran insect flight dynamics. part 1 longitudinal motion about hover," *Journal of theoretical biology*, vol. 264, no. 2, pp. 538–552, 2010.

[20] B. Cheng and X. Deng, "Translational and rotational damping of flapping flight and its dynamics and stability at hovering," *IEEE Transactions On Robotics*, vol. 27, no. 5, pp. 849–864, 2011.

[21] H. E. Taha, C. A. Woolsey, and M. R. Hajj, "Geometric control approach to longitudinal stability of flapping flight," *Journal of Guidance Control and Dynamics*, vol. 39, no. 2, pp. 214–226, 2016.

[22] A. Hassan and H. Taha, "Differential-geometric-control formulation for flapping flight multi-body dynamics," *Submitted to Journal of Nonlinear Sciences*.

[23] R. J. Wood, "The first takeoff of a biologically inspired at-scale robotic insect," *IEEE Transactions on Robotics and Automation*, vol. 24, no. 2, pp. 341–347, 2008.

[24] "Gravity 360 degree hall angle sensor," https://www.dfrobot.com/wiki/index.php/Gravity:_Hall_Angle_Sensor_SKU:_SEN0221.

[25] "Diy electric dove super capacitor wing flapping bird toy gift," https://www.banggood.com/Wing-Flapping-Bird-Toy-Gift-p-1013167.html.

[26] "Nano qx 6x15mm ballistic 19,600kv," https://www.

amazon.com/Apex-RC-Products-Inductrix-Ballistic/dp/B0711251VV/ref=pd_ybh_a_52?_encoding=UTF8&psc=1&refRID=NASVAW8SBAW1Z82R4CXW.

[27] "Object detection - color filtering - opencv - c++," http://jematoscv.blogspot.com/search/label/Projects.

[28] C. P. Ellington, "The aerodynamics of hovering insect flight: Ii. morphological parameters," *Philosophical Transactions Royal Society London Series B*, vol. 305, pp. 17–40, 1984.

[29] J. H. Wu, Y. L. Zhang, and M. Sun, "Hovering of model insects: simulation by coupling equations of motion with navier-stokes equations," *The Journal of Experimental Biology*, vol. 212, no. 20, pp. 3313–3329, 2009.

[30] H. E. Taha, M. R. Hajj, and A. H. Nayfeh, "On the longitudinal flight dynamics of hovering mavs/insects," *Journal of Guidance Control and Dynamics*, vol. 37, no. 3, pp. 970–978, 2014.

[31] A. Banazadeh and N. Taymourtash, "Adaptive attitude and position control of an insect-like flapping wing air vehicle," *Nonlinear Dynamics*, pp. 1–20, 2016.

[32] A. Stephenson, "On an induced stability," *The London, Edinburgh, and Dublin Philosophical Magazine and Journal of Science*, vol. 15, no. 86, pp. 233–236, 1908.

[33] J. M. Berg and I. M. Wickramasinghe, "Vibrational control without averaging," *Automatica*, vol. 58, pp. 72–81, 2015.